

## An integrated elastomer substrate with a lens array and pixel elements for three-dimensional liquid crystal displays

Jong-Ho Hong, Yeun-Tae Kim, Yunhee Kim, Byoung-ho Lee and Sin-Doo Lee\*

*School of Electrical Engineering, #032 Seoul National University, Kwanak, PO Box 34, Seoul 151-600, South Korea*

*(Received 5 January 2012; Revised 19 January 2012; Accepted for publication 30 January 2012)*

In this paper, a concept of an integrated elastomer substrate for a three-dimensional (3D) liquid crystal display based on the integral-imaging method is presented. The elemental lens array and columnar spacers were integrated into one of the two substrates, an elastomer substrate, through an imprinting process. The integrated elastomer substrate was capable of maintaining the uniform liquid crystal (LC) cell gap and promoting homeotropic LC alignment without any surface treatment. The monolithic approach reported herein will provide a key component for 3D displays with enhanced portability through a more than 40% weight reduction compared with the conventional integral-imaging method.

**Keywords:** three-dimensional display; integrated elastomer substrate; integral imaging; imprinting technique

### 1. Introduction

A three-dimensional (3D) display technology has been considered as the ultimate goal for future displays because it provides more realistic images with in-depth information that cannot be realized in the conventional two-dimensional (2D) case. The 3D displays have great potential for various fields, such as in television, games, medical imaging, education, and military applications. Several methods have been developed for producing 3D images, such as the holographic method [1,2], the lenticular-lens method [3,4], the parallax barrier method [5,6], and the integral-imaging method [7,8]. Among these, the integral-imaging method, which employs a lens array to create 3D images from synthetic 2D elemental images, has been studied quite extensively because of its capability of providing full-parallax, full-color moving pictures, its quasi-continuous viewing points within a certain viewing angle range, and its relatively small 3D viewing fatigue. Generally, an integral-imaging system consists of an elemental-lens array and an image display device, such as a liquid crystal (LC) panel or a beam projector. In the case of the LC panel, however, the fabrication of an integral-imaging display needs accurate aligning and assembling processes for bonding the external lens array in front of the LC panel. Moreover, such an external lens array increases the weight and the cost of manufacturing the 3D display system.

In this paper, a concept of the integrated elastomer substrate with a lens array [9] for 3D displays based on the integral-imaging method is introduced.

The integrated elastomer substrate, fabricated using an imprinting technique, serves as a monolithic substrate with a lens array for constructing 3D images on the outer surface and with columnar spacers for maintaining the uniform LC cell gap on the inner surface. Moreover, the monolithic substrate spontaneously produces homeotropic LC alignment without any surface treatment. The proposed 3D LC cell shows good 3D images with different parallaxes varied in the viewing angle of about  $17^\circ$  and reduces the weight by about 40% compared with the conventional integral-imaging case.

### 2. Concept of a 3D LC cell with an integrated elastomer substrate

Figure 1(a) shows a schematic diagram of a conventional 3D liquid crystal display (LCD) using the integral-imaging method, which consists of an LC panel and a lens array for constructing 3D images from 2D elemental images. In this configuration, a sheet of plastic lens array needs to be assembled in front of the LC panel with precise alignment, using a bonding layer. Figure 1(b) shows the proposed 3D LCD constructed with an integrated elastomer substrate as the top substrate, which contains both a lens array and columnar spacers. The proposed approach has several advantages over the existing technologies in fabricating a 3D LCD, based on the integral-imaging method. For example, the aligning and assembling processes between the lens array and the top substrate are not necessary. The uniform cell

---

\*Corresponding author. Email: sidlee@plaza.snu.ac.kr

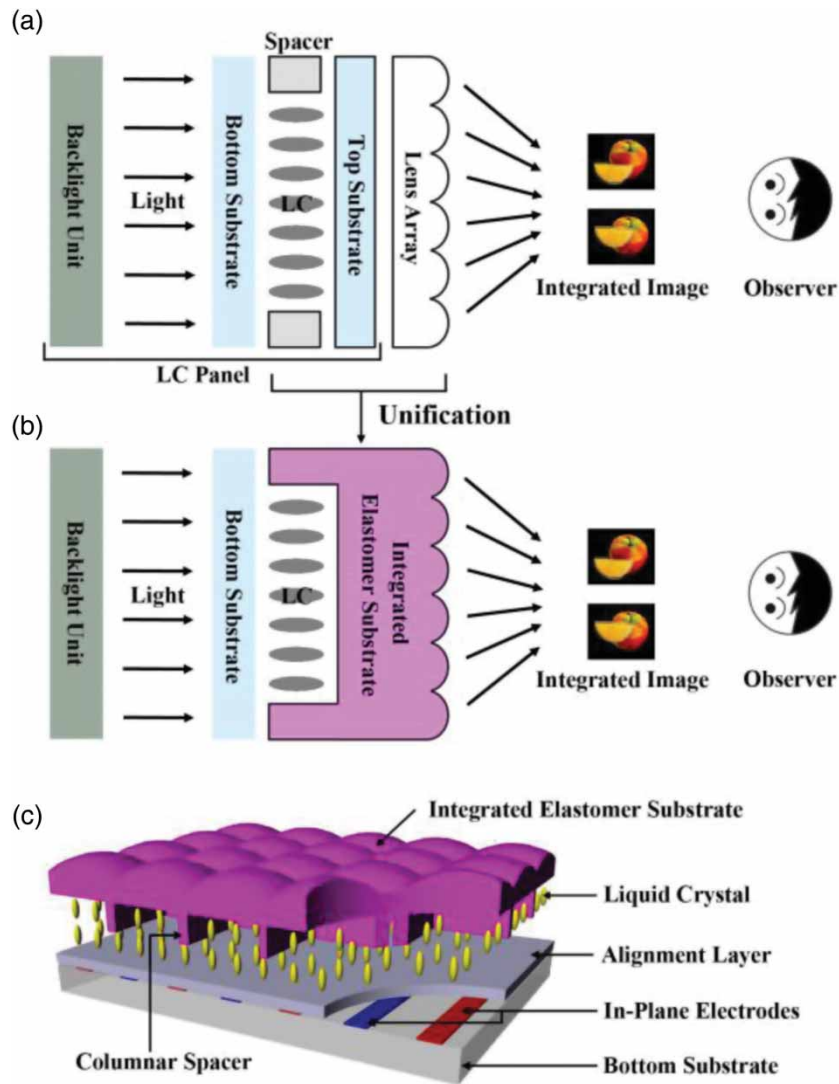


Figure 1. Schematic diagrams showing the 3D LCD based on the integral-imaging method: (a) a conventional configuration, (b) the proposed configuration using an integrated elastomer substrate, and (c) the proposed 3D LC cell using an integrated elastomer substrate as a top substrate.

gap is simply maintained by the columnar spacers, and the homeotropic LC alignment is spontaneously promoted by the intrinsic nature of the elastomer surface. Such multifunctionality of the elastomer substrate enables the construction of a new-concept transmissive LCD [10] or a flexible LCD [11].

### 3. Fabrication of an integrated elastomer substrate

The imprinting technique [12–14] was employed for fabricating the integrated elastomer substrate using two different molds, I and II, as shown in Figure 2(a). It has been widely used for duplicating the 3D geometric shapes stored in a mold through a single-step process. The elastomeric material of polydimethylsiloxane (PDMS) of Sylgard 184 (Dow Corning) was used for the integrated elastomer substrate. Note that PDMS is an optically isotropic, transparent,

flexible, and durable material that is appropriate for the substrate of an LC panel. PDMS was first poured onto mold II and was subsequently pressed using mold I, giving the film thickness  $t = 3.35$  mm. After the curing of the PDMS film for 90 min at  $150^{\circ}\text{C}$ , the film was peeled off from the two molds, as shown in Figure 2(a). Then, the outer and inner surfaces of the integrated elastomer substrate helped the lens array to generate 3D images and the columnar spacers to maintain a uniform cell gap, respectively. Scanning electron microscope (SEM) images of the two surfaces of the integrated elastomer substrate are shown in Figure 2(b). The physical dimensions of the pitch and the maximum height of the single lens structure were 995 and  $75\ \mu\text{m}$ , respectively. The width, height, and interval of the columnar spacers were 30, 5, and  $300\ \mu\text{m}$ , respectively. Compared with a typical substrate, such as glass or a plastic film, which requires the LC alignment process, the integrated elastomer

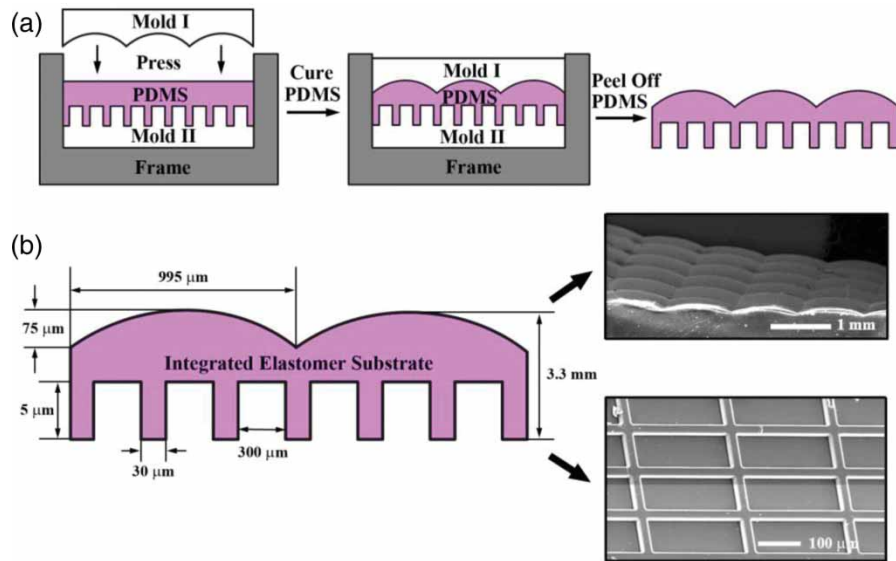


Figure 2. Fabrication processes and microstructures (lens array and columnar spacers) of an integrated elastomer substrate: (a) fabrication processes of an integrated elastomer substrate by imprinting an elastomeric material (PDMS) between two different molds and (b) physical dimensions of the lens array on the outer surface and of the columnar spacers on the inner surface in the integrated elastomer substrate together with the SEM images.

substrate used as the top substrate homeotropically aligns the LC molecules without any surface treatment due to its hydrophobic nature and low surface energy. The bottom substrate, which had in-plane electrodes, was coated with an LC alignment layer of JALS 684 (Japan Synthetic Rubber Co.) for homeotropic LC alignment. The LC material that was used in this work was ZLI-2293 (Merck), whose birefringence  $\Delta n$  and dielectric anisotropy  $\Delta\epsilon$  were 0.1322 and 10, respectively.

#### 4. Results and discussion

The electro-optic (EO) properties of the LC cell constructed with the integrated elastomer substrate were examined first. Figure 3 shows the microscopic textures and the focused

light images of the LC cell at different applied voltages. The experimental setup consisted of a polarizing optical microscope (Nikon OptiphotII-pol), the LC cell with the integrated elastomer substrate, crossed polarizers whose optic axes were made at an angle of  $45^\circ$  with respect to the direction of the electrode stripes, and a white light source. In the absence of an applied voltage, a dark state was obtained in each pixel element, as shown in Figure 3(a), indicating that the LC molecules were vertically aligned. In other words, the integrated elastomer substrate is indeed capable of producing homeotropic LC alignment without any surface treatment. In the presence of an applied voltage, the LC molecules were reoriented along the in-plane electric field, and light was transmitted through the LC cell due to the phase retardation of the LC layer, as shown in

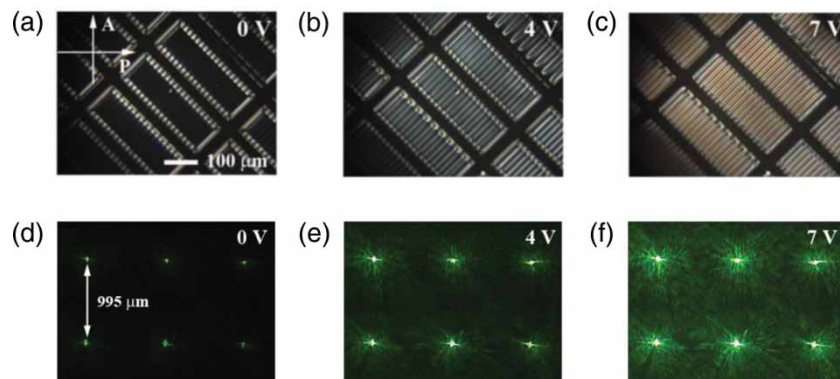


Figure 3. Microscopic textures of the pixel elements in the proposed LC cell with in-plane electrodes in the homeotropic configuration at different applied voltages: (a) 0 V, (b) 4 V, and (c) 7 V. Intensity variation of the focused light through the lens array in the LC cell at different applied voltages: (d) 0 V, (e) 4 V, and (f) 7 V.

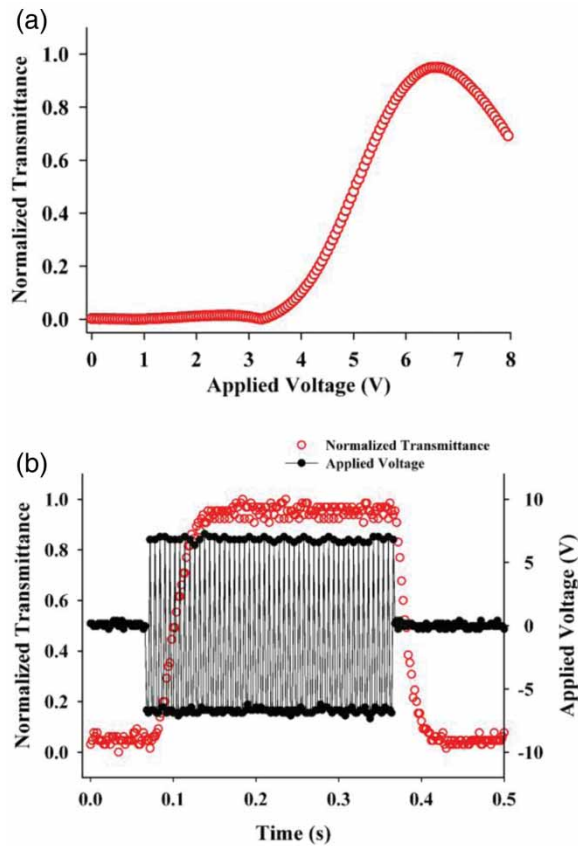


Figure 4. EO transmission and response of the LC cell: (a) normalized transmittance as a function of an applied voltage and (b) dynamic response at the applied voltage of 7 V.

Figure 3(b) and (c). The intensity variation of the focused light through the lens array was measured using an He–Ne laser with a 543.5 nm wavelength. The brightness through the focused region in each pixel element was varied with

the applied voltage, as shown in Figure 3(d)–(f). The focal length was determined to be about 3.35 mm, which is comparable to the film thickness  $t$  of the integrated elastomer substrate. Note that a small amount of light leakage will inevitably occur near the columnar spacers in the absence of the applied voltage. This light leakage can be minimized by reducing the physical dimensions of the columnar spacers.

The normalized EO transmittance and the response times of the LC cell are shown in Figure 4(a) and (b), respectively. The EO properties of the region of  $3 \times 3$  pixels were measured using an He–Ne laser with a 632.8 nm wavelength in the presence of a square-wave bipolar voltage at a frequency of 1 kHz. The threshold voltage was about 3.2 V. The EO transmittance reached the maximum at 6.5 V and decreased with the further increase of the applied voltage due to the phase retardation beyond  $\pi$ , as shown in Figure 4(a). The contrast ratio was found to be about 80:1. In Figure 4(b), the open circles (red) and the black line represent the EO response of the LC cell and the applied voltage, respectively. It was found that at the applied voltage of 7 V, the rising time was about  $38 \pm 2$  ms and the falling time was about  $25 \pm 2$  ms. It should be noted that a few tens of milliseconds of the measured switching speed resulted mainly from the LC material properties and not from the limitation of the integrated elastomeric substrate.

The lens array part of the integrated elastomer substrate was applied to a commercial LC panel to simply characterize the 3D imaging performance of the lens array shown in Figure 2(b). The commercial LC panel was 15 in. diagonally (GH15US, Samsung Electronics), and its active display region was  $4 \times 3$  in<sup>2</sup>. The 3D LCD that was used in the experiment consisted of a commercial LC panel, a lens array, and two polarizers in the focused-mode integral-imaging configuration, as shown in Figure 5(a).

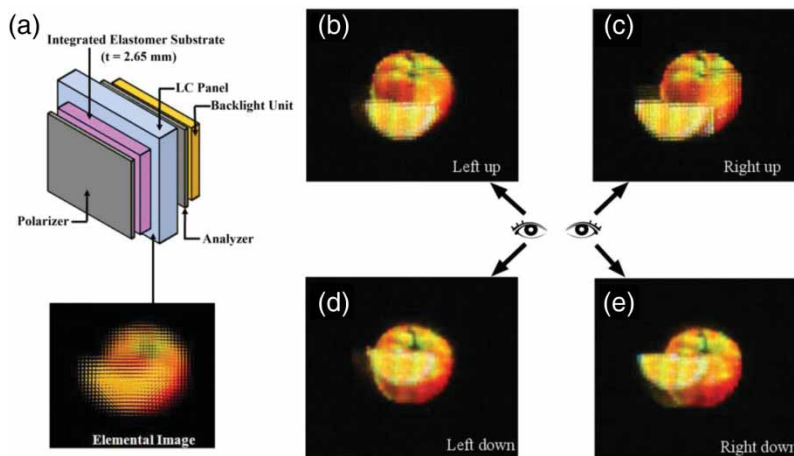


Figure 5. (a) Schematic diagram of the 3D LCD system with a lens array in the elastomer substrate placed on a commercial LC panel that displays a computer-generated elemental image. Camera-captured 3D images observed along four different viewing directions: (b) left up, (c) right up, (d) left down, and (e) right down diagonally at the polar angle of  $15^\circ$ .

Taking into account the thickness (0.7 mm) of the front glass substrate of the LC panel, the effective thickness of the elastomer substrate with the lens array was considered to be  $t = 2.65$  mm. The experimental results obtained for the 3D images (an apple and an orange) captured using a digital camera (Sony, A300) when a computer-generated elemental image is displayed on the 3D LCD are shown in Figure 5. Different 3D images along four different observation directions (left up, right up, left down, and right down diagonally) at the polar angle of  $15^\circ$  are shown in Figure 5(b)–(e), respectively. In general, the viewing angle ( $\omega$ ) at which an observer can see the complete 3D images is given by  $\omega = 2 \tan^{-1}(p/2t)$ , where  $p$  is the pitch of an elemental lens (assuming that the horizontal and vertical pitches are equal) and  $t$  is the gap between the lens array and the elemental image of the display panel. The calculated viewing angle was then estimated as  $17.2^\circ$  using the parameters  $p = 0.99$  mm and  $t = 3.35$  mm. Note that the 3D architecture based on the integrated elastomer substrate can be easily extended to a curved integral-imaging system [8] so that the viewing angle can be enhanced up to  $66^\circ$ .

## 5. Conclusion

In this paper, a 3D LCD with an integrated elastomer substrate based on the integral-imaging method has been described. The integrated elastomer substrate fabricated through the imprinting technique has the self-aligning capability of the LC molecules and two types of surface microstructures, one of which is a lens array for producing 3D images and the other columnar spacers for maintaining a uniform LC cell gap on the inner surface. Recently, efforts have been made to commercialize large PDMS elements via soft lithography [15]. For example, micropatterned PDMS light guide plates have been demonstrated for LCD applications [16]. The proposed 3D architecture using an integrated elastomer substrate will provide better portability and durability and will allow the cost-effective manufacturing of future 3D displays.

## Acknowledgement

This work was supported by Samsung Electronics Co., Ltd.

## References

- [1] S. Tay, P.-A. Blanche, R. Voorakaranam, A.V. Tunc, W. Lin, S. Rokutanda, T. Gu, D. Flores, P. Wang, G. Li, P.St. Hilaire, J. Thomas, R.A. Norwood, M. Yamamoto, and N. Peyghambarian, *Nature* **451**, 694 (2008).
- [2] P.St. Hilaire, S.A. Benton, and M. Lucente, *J. Opt. Soc. Amer. A* **9**, 1969 (1992).
- [3] Y.-G. Lee and J.B. Ra, *Opt. Eng.* **45**, 017007 (2006).
- [4] O.H. Willemsen, S.T.De. Zwart, M.G.H. Hiddink, and O. Willemsen, *J. Soc. Inf. Disp.* **14**, 715 (2006).
- [5] H.J. Park, Y.B. Lee, J.H. Woo, K.B. Park, and W.S. Kim, in *Proceedings of 15th International Display Workshops*, Niigata Convention Center, Niigata, Japan, 2008, pp. 1165–1166.
- [6] H. Nishimura, H. Yamamoto, and Y. Hayasaki, in *Proceedings of 14th International Display Workshops*, Sapporo Convention Center, Sapporo, Japan, 2007, pp. 1173–1176.
- [7] J.-H. Park, H.-R. Kim, Y. Kim, J. Kim, J. Hong, S.-D. Lee, and B. Lee, *Opt. Lett.* **29**, 2734 (2004).
- [8] Y. Kim, J.-H. Park, S.-W. Min, S. Jung, H. Choi, and B. Lee, *Appl. Opt.* **44**, 546 (2005).
- [9] Y.-T. Kim, J.-H. Hong, J.-H. Na, Y. Kim, B. Lee, and S.-D. Lee, in *Proceedings of SID Symp. Dig.* Seattle Convention Center, Seattle, Washington, DC 2010, pp. 946–948.
- [10] Y.-T. Kim, J.-H. Hong, S.-M. Cho, and S.-D. Lee, *J. Inf. Disp.* **10**, 68 (2009).
- [11] Y.-T. Kim, J.-H. Hong, T.-Y. Yoon, and S.-D. Lee, *Appl. Phys. Lett.* **88**, 263501 (2006).
- [12] Y. Xia and G. M. Whitesides, *Angew. Chem., Int. Ed.* **37**, 550 (1998).
- [13] L.J. Guo, *J. Phys. D: Appl. Phys.* **37**, R123 (2004).
- [14] S.Y. Chou, P.R. Krauss, and P.J. Renstrom, *J. Vac. Sci. Technol. B.* **14**, 4129 (1996).
- [15] J.A. Rogers and R.G. Nuzzo, *Mater. Today* **8**, 50 (2005).
- [16] J.-H. Lee, H.-S. Lee, B.-K. Lee, W.-S. Choi, H.-Y. Choi, and J.-B. Yoon, *Opt. Lett.* **32**, 2665 (2007).